

Article

Adoption of Multiphase and Variable Flux Motors in Automotive Applications

Beñat Arribas ^{*} , Gaizka Almandoz , Aritz Egea , Patxi Madina  and Ion Iturbe 

Faculty of Engineering, Mondragon Unibertsitatea, 20500 Arrasate-Mondragón, Spain;
galmandoz@mondragon.edu (G.A.); aegea@mondragon.edu (A.E.); pmadina@mondragon.edu (P.M.);
iiturbeb@mondragon.edu (I.I.)

* Correspondence: barribas@mondragon.edu; Tel.: +34-678-360-115

Abstract: This paper investigates the incorporation of multiphase (MP) and variable flux (VF) permanent magnet motors to electric vehicles (EVs). A literature review is carried out first, which covers the characteristics, benefits and challenges of both motor configurations. MP motors, with their increased phase number, offer enhanced fault tolerance, reduced torque ripple, and improved efficiency, among other benefits. VF technology allows for dynamic adjustment of the magnetic field, optimising motor performance across various operating conditions. By integrating these technologies, this study aims to harness the benefits of both MP configurations and VF capabilities. For this reason, the Finite Element Method (FEM) is used with three-phase, MP, VF, and VF-MP motors. The main contribution is that both technologies have been implemented in a single motor to evaluate and quantify their impact together, obtaining higher torque and constant power values, lower torque ripples, and higher efficiencies in the whole working range.

Keywords: multiphase; variable flux; permanent magnet motor; Finite Element Method (FEM); electric vehicle (EV)



Citation: Arribas, B.; Almandoz, G.; Egea, A.; Madina, P.; Iturbe, I. Adoption of Multiphase and Variable Flux Motors in Automotive Applications. *Appl. Sci.* **2024**, *14*, 10932. <https://doi.org/10.3390/app142310932>

Academic Editors: Gang Lei, Youguang Guo, Jianguo Zhu, Yujiao Zhang and Bo Ma

Received: 24 October 2024
Revised: 15 November 2024
Accepted: 22 November 2024
Published: 25 November 2024



Copyright: © 2024 by the authors. Licensee MDPI, Basel, Switzerland. This article is an open access article distributed under the terms and conditions of the Creative Commons Attribution (CC BY) license (<https://creativecommons.org/licenses/by/4.0/>).

1. Introduction

The transition towards electric transportation has been driven by concerns about climate change and global warming. This shift has resulted in a surge in the sales of electric vehicles (EVs), stimulating a wealth of research in this field. The motor of an electric vehicle has a direct impact on autonomy, which is a key hurdle in the transition to electric transportation. Thus, the development of efficient and power-dense motors can contribute to reducing costs and enhancing vehicle autonomy.

The trend towards higher speeds is evident in the evolution of the Toyota Prius, as discussed by Okamura et al. [1]. Higher speeds result in lower torque requirements for a given power, enabling a reduction in motor size [2]. Additionally, increased speeds demand higher switching frequencies, making wide band-gap semiconductors promising candidates for electric vehicle inverters [3]. Regarding motor topologies, permanent magnet motors are predominantly used due to their superior power densities and efficiencies, as shown in the market analysis by El Hadraoui et al. [4]. However, induction motors (e.g., Tesla Model S) and electrically excited motors (e.g., Renault ZOE) are also used [5].

In recent investigations, multiphase (MP) permanent magnet motors have been suggested as a feasible option for electric vehicles, offering several advantages over the standard three-phase motors. These include higher torque density, lower torque ripple, power segmentation, and improved fault tolerance [6–8]. Moreover, several studies demonstrate that higher efficiency and power density can be obtained with MP motors compared to their three-phase counterparts [7,9]. MP motors are already being implemented in market EVs, but their presence remains limited due to the simplicity and cost-effectiveness of the well-established 3-phase motors [10]. DANA TM4 offers 6- and 9-phase motors ranging from 100 kW to 430 kW of continuous power, which are used in EMOSS trucks (6-phase

200 kW/950 Nm and 9-phase 250 kW/3400 Nm) [10,11]. The BMW iX M60 is another example, featuring a 6-phase motor with an electrically excited rotor [4]. Additionally, companies such as Mercedes are dedicating part of their research to MP motors [10,12]. Although 3-phase motors currently dominate the EV market, MP motors are gaining interest due to their high potential.

Variable flux (VF) motors have also been shown to improve efficiency and torque-speed capability. These motors have several mechanisms for adjusting the permanent magnet flux, which can maximise efficiency in each working point. In fact, a number of authors have found that high levels of efficiency are obtained in the whole working region [13–15]. Although the academic interest in these motors is increasing, no commercial examples were found.

It is clear that the interest in MP and VF motors is increasing, and Gholamian et al. [16] recently reviewed multiphase motors together with hybrid excitation ones, these last being one type of VF motors. However, no published comparison between both motor types has been found. Therefore, the improvement in performance of both topologies has not been clearly quantified. Moreover, although studies such as [17,18] propose multiphase hybrid excited variable flux motors, up to now, far too little attention has been paid to multiphase variable flux permanent magnet motors, which could combine the advantages of both.

This article, therefore, identifies and compares the benefits and drawbacks of each topology. To this end, a literature review of MP and VF motors is conducted, in which the main characteristics and design challenges are addressed. Then, to quantify improvements in motor performance, an automotive three-phase motor is taken as a reference, and it is modified to obtain equivalent MP, VF, and MP-VF motors. Then, these three design alternatives are compared to the reference three-phase motor in terms of torque and power capability, efficiency, and torque ripple, using the Finite Element Method (FEM). The main contribution is that both technologies have been implemented in a single motor to evaluate and quantify their impact together, obtaining higher torque and constant power values, lower torque ripples, and higher efficiencies in the whole working range.

2. Literature Review

2.1. Multiphase Motors

In recent years, MP motors have attracted special interest in the automotive sector, which has resulted in considerable research on this topic. MP motors are motors with more phases than traditional three-phase ones, which delivers several advantages. The fault tolerance of these motors is of particular interest to EVs, but they also feature higher power density, reduced torque pulsation, power segmentation, and more degrees of freedom for control purposes [9,10,19–21]. Their main advantages and challenges to incorporate to EVs are explained in more detail below.

2.1.1. Impact of MP Motors on the Inverter

One of the advantages of having multiphase motors in EVs is the power segmentation. In automotive converters for three-phase motors, the semiconductors are paralleled to satisfy the electric current requirement (the higher the power, the greater the need for paralleling). The need for paralleling is even greater with new wide band-gap (WBG) devices, as their current rating is lower than in silicon Insulated Gate Bipolar Transistors (IGBTs), mainly because of reduced die size. A clear example is the Tesla Silicon Carbide (SiC) inverter, in which four Metal Oxide Semiconductor Field Effect Transistors (MOSFET) are paralleled in each inverter branch [22]. Paralleling is not an easy task and can lead to a less efficient and less reliable system [23,24]. For this reason, in [7], an MP drive was proposed to overcome this parallelisation problem in a 50 kW drive. The total power was split into 21 phases, with the result that each semiconductor withstood less current, and avoiding the need for paralleling.

As regards inverter size, DC-link capacitance is one of the bulkiest elements in the converter, and can be around 2/3 of the total size. With MP drives, the capacitance and

current requirements of DC-link capacitors are lowered. This allows the use of smaller capacitors and increases the power density of the converter while reducing its cost [10,11]. Taha et al. mention that a reduction of 50% in capacitance and 10% in DC bus Root Mean Square (RMS) current is achieved by increasing the phase number from 3 to 6 [25].

The primary challenge with inverters is that three-phase inverters are significantly more common and cheaper than MP inverters. Consequently, three-phase inverters are available in a variety of voltage and power ratings, unlike multiphase inverters. To address this issue, dual three-phase (DTP) drives have been proposed for electric vehicles, offering a more cost-effective solution [26]. Two three-phase inverters can be used in parallel to feed a dual three-phase motor, benefiting from the advantages of MP drives while using conventional three-phase inverters.

2.1.2. Performance of MP Motors

Multiphase motors have several benefits over the three-phase ones. Many authors confirmed the higher torque capability of multiphase motors due to an increase in the winding factor. Wang et al. adapted the Toyota Prius 2010 motor from three-phase to DTP, obtaining a 3.53% higher winding factor and a 2.45% higher maximum torque [27]. In [28], a fractional 12 slot and 10 pole motor was analysed and 3.5% higher torque was obtained.

In terms of torque ripple, increasing the number of phases reduces torque ripple [6,29]. In [27], torque ripple was reduced more than 60%, and in [28], around 18%. Moreover, as analysed in [30], the order of the first torque ripple harmonic increases. In the case of DTP motors with phase displacement of 30°, the order of the first torque ripple harmonic increases from 6 to 12 [31].

When it comes to efficiency and power losses, the more sinusoidal magnetomotive force of multiphase motors reduce iron losses. Abdel-Khalik et al. observed 24%, 44%, and 60% reductions in stator iron, magnet, and rotor iron losses, respectively, in the DTP motor compared to the equivalent three-phase one [28]. Alternatively, Keller et al. noticed a higher continuous power capability in an automotive motor and a 3% higher efficiency over the WLTC driving cycle [12], which was partly thanks to the higher winding factor.

On the other hand, the higher number of phases brings the opportunity to use the additional degrees of freedom for different purposes, some of which are listed and explained below:

- **Current harmonic injection (CHI):** To increase torque in MP motors, higher-order current harmonics can be used. The idea is to use the higher-order EMF harmonics to produce torque by injecting the corresponding current harmonics, the same way it is achieved with the fundamental one. The torque capability of five-phase [29,32,33], DTP [34,35], seven-phase [36], and nine-phase [37] motors is addressed in the articles, while in [38] asymmetric motors were analysed. In [39] and [40], the permanent magnet shape of a surface permanent magnet DTP motor was analysed. By changing the magnet shape and injecting current harmonics (3rd, 5th, and 7th), torque was improved by 30%. Additionally, Sculler et al. [36] designed a seven-phase motor with simultaneously 2 and 6 pole pairs taking advantage of this characteristic.
- **Fault-tolerant controls:** Fault tolerance is interesting for automotive motors. After a fault, the additional degrees of freedom can be used to continue operating. Controls with different objectives can be distinguished in the literature, such as the minimisation of copper losses [41], the balancing of current waveform amplitudes [8], and torque ripple minimisation [42]. Moreover, according to [43], robust controllers such as the Fuzzy Logic Controller can deal with motor faults even without fault detection. This was demonstrated in [44] for a nine-phase induction motor.
- **Multimotor operation:** Various motors can operate with a single inverter, referred to in the literature as multimotor operation [21,45]. This is achieved by phase transposition, which allows each motor to operate in different $\alpha\beta$ planes as the phase sequence of the motors is different. However, this operating mode is not interesting for electric vehicles, as copper losses would be double.

2.2. Variable Flux Motors

To have a wider torque–speed envelope and more efficient high-speed performance, VF motors have been suggested in the literature in the last few years. The objective with these motors is to somehow vary the permanent magnet flux linkage to operate with different flux levels at different regions, thus obtaining good performance at low speed as well as high speed, as illustrated in Figure 1, where the circles inside the envelopes represent the highest-efficiency regions.

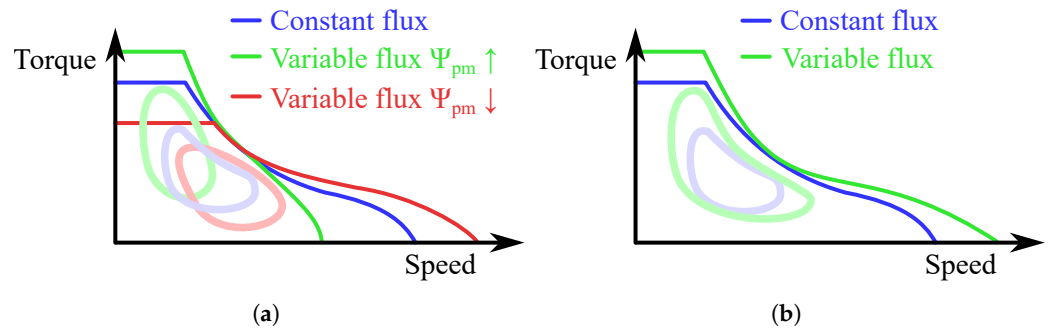


Figure 1. Torque–speed envelope and high-efficiency zone improvement with VF motors. (a) Envelope with different flux levels. (b) Overall operation envelope.

Several publications review the different ways to achieve a variable flux [46–49]. They agree that there are three main ways to obtain a variable flux field. Using hybrid excitation (HE) motors is the most known one, where the field windings allows to adjust the flux linkage. Another way to vary the flux linkage is by demagnetising and magnetising low coercive field magnets. Last, flux can be mechanically varied in different ways. Next, the three motor types will be reviewed.

2.2.1. Hybrid Excitation Motors

HE motors have extra field coils (FCs) apart from the stator winding and rotor permanent magnets (PMs) compared to traditional PM motors. These FCs enhance or weaken the permanent magnet flux by applying a DC current.

A great amount of different topologies exist among the HE motors. One main separation is made in [50] according to the location of the magnets and field windings, which can be either in the rotor or in the stator. Figure 2 shows an example of each.

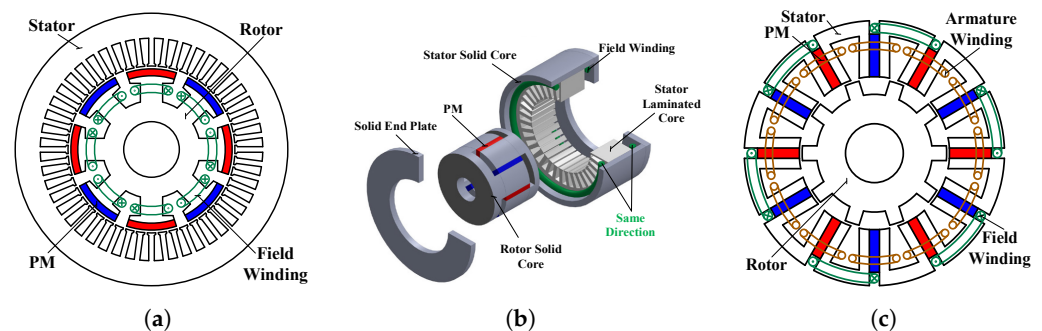


Figure 2. HE motor types depending on magnet and field coil location [50]. (a) PM: rotor/FC: rotor. (b) PM: rotor/FC: stator. (c) PM: stator/FC: stator.

Topologies with PMs and FCs in the rotor (Figure 2a) can be formed by mixing FCs and PMs in the rotor. This way, the stator remains the same, but electric energy has to be transmitted to the rotor, which usually requires slip rings, increasing maintenance cost and making the system less reliable. In [51], the flux-weakening capacity was notably improved by adding field coils in the rotor of an IPM motor. In addition, in [52], the torque density was increased by adding permanent magnets to an electrically excited rotor. Unlike other

alternatives, in [53], by changing the polarity of field coils, the motor could work as a 4-pole or as a 8-pole one, which was useful to widen the speed range.

Using different flux paths for magnets and field coils, that is, using parallel magnetic circuits for magnets and field coils, it is possible to move the field coils to the stator as shown in Figure 2b. This way, there is no need to feed the rotor, eliminating the slip rings. In [54], some configurations with field coils in the stator are presented. It is stated that some of them needed extra yokes in the axial flux path, making the motor heavier, as the example in Figure 2b. The motor in [55], additionally, needed an extra stator yoke for the circulation of field coil flux, and part of the rotor was not used. Therefore, HE motors having the field coil in the stator do also have some drawbacks.

Another option is to put the magnets as well as the FCs in the stator. Among these motors, the flux switching [56,57] and flux reversal [58] topologies can be adopted, as they have PMs in the stator. By adding FCs in the stator, permanent magnet flux can be enhanced or weakened the same way it is accomplished with the other alternatives. Additionally, in [59], a hybrid claw pole motor was adopted, but the PM location was changed from the rotor to the motor front and back covers, to generate axial flux. This allowed it to avoid problems in the magnets due to the centrifugal force in high-speed motors, but increased the reluctance of the magnetic circuit of the field coil, as it was arranged in series with the PMs.

To sum up, HE motors obtain a better flux-weakening capability than IPM motors but need extra elements such as field coils, power supply, and flux paths, making the manufacturing process more complex, increasing the mass of the motor, and making it more expensive. These are the main limiting points for not adopting them in market EVs.

2.2.2. Variable Flux Memory Motors

Variable flux memory motors (VFMMs) make use of low-coercivity magnets (LCMs) together with high-coercivity magnets (HCMs) to adjust the PM flux. HCMs remain magnetised in the whole working range the same as in traditional permanent magnet motors, whereas LCMs are demagnetised and magnetised by applying d -axis current pulses to manipulate the magnetisation state (MS), in this way extending the operating range and efficiency of the motor [60]. The main advantage of these motors is that they do not need any extra elements such as field coils, which is beneficial from manufacturing point of view.

With the magnetisation state manipulation, higher efficiencies are achieved. Yang et al. observed a maximum of 17% of efficiency improvement at high speed and low torque compared to the Nissan Leaf IPM motor. Athavale et al. evaluated motors between 120 kW and 275 kW at different drive cycles, and achieved power loss reductions between 14% and 28%. Additionally, the survey paper by Jayarajan et al. [61] demonstrates the possibility to extend the maximum torque–speed envelope of the motor.

One of the main drawbacks is the high demagnetising and magnetising currents required to change the MS of the LCMs. In fact, Badahdah and El-Refaie state that it is the biggest challenge to obtain competitive VFMMs [62]. The inverter must be oversized to provide these currents, which are typically several times the working current [63]. Han et al. report that 2.5 p.u. and 6.5 p.u. currents are needed to demagnetise and magnetise LCF magnets, respectively [64]. Similarly, the work [65] states that 800 A and 1600 A are required for a 325 A motor. Reducing these currents limits the range of manipulation of the MS, and a compromise must be made according to [66]. Moreover, decreasing the demagnetising current can lead to unwanted demagnetisation.

To balance the magnetising and remagnetising currents, the rotor topology and the magnet arrangement are the key points according to Yang et al. [67]. They state that the magnetising current is very high in the parallel configuration, and it can suffer from unwanted demagnetisation due to the low demagnetising current (confirmed in [64]). Meanwhile, the demagnetising current is increased higher in the series one, avoiding unwanted demagnetisation, but requiring larger currents for MS manipulation (confirmed

in [68]). Therefore, Yang et al. propose a hybrid configurations to balance both currents. Figure 3, based on [67], shows three possible magnet configurations, series, parallel, and hybrid, together with the load curves of the LCMs.

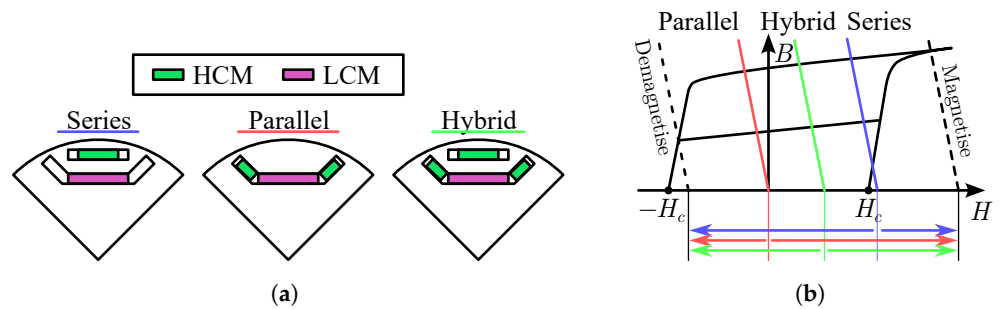


Figure 3. Series, parallel and hybrid magnetic configurations in VFMM rotor. Based on [67]. (a) Magnet arrangements. (b) LCM load curves.

To address the unwanted demagnetisation problem, some of the authors opt for flux-intensifying configurations. The idea is that, in these motors, the MTPA curve is located in the first quadrant of the I_d - I_q plane as $L_d > L_q$, thus operating with positive d -axis current and avoiding the risk of demagnetisation in normal operation. In [69], the motor can operate until 90% of full load condition without unwanted demagnetisation, and the MS control current needed is 4 p.u.

All in all, the VFMM is a potential candidate for electric vehicles as they substantially improve the efficiency, especially at high speeds. However, the problem of large MS control currents has to be solved as the oversizing of the inverter is too high in all cases.

2.2.3. Mechanically Flux-Varying Motors

Adjusting the flux linkage mechanically is the remaining option to obtain a variable flux motor. One way is to use externally controlled mechanical actuators, and the other is to take advantage of the centrifugal force at high speed to somehow change the flux. Different flux-weakening mechanisms are proposed in the literature.

Mechanisms that use the centrifugal force of the rotor as actuator normally use springs to activate the flux-weakening mode. The motors of [70–73] use springs in the end-plates of the rotor to rotate the magnets in the rotor and in this way vary the linked flux. In [74], the magnetic circuit of a spoke-type motor is short-circuited in the inner part of the rotor thanks to a clutch that is activated at a given speed. When it comes to [75], a flux-weakening mechanism is presented for a double-rotor axial flux motor. An actuator with springs in one of the rotors allows it to shift the angle with respect the other rotor, which is equivalent to skewing a rotor, which allows it to obtain the flux-weakening effect. Although additional mechanisms are needed in all the configurations, their main advantage is that no external input is needed to activate the actuators.

The mechanisms that use the centrifugal force to activate the flux-weakening mode are located in the rotor, as this is the moving part. When it comes to externally activated actuators, they can be located in the stator, in the rotor, or even in the airgap.

Liu et al. suggested in [76] a novel flux-switching motor where the magnets are located in an iron ring in the airgap. When this permanent magnet iron ring is rotated, the flux linkage can be adjusted. In [77], a similar iron ring mechanism is used for a spoke-type motor. By aligning the magnetic conducting parts of the ring with the stator teeth, the maximum flux linkage is obtained, and vice versa.

An example of a flux-varying motor with the actuator in the stator is presented in [78,79]. The same as in some other cases, the basis of the mechanism consists of short-circuiting the magnet flux to reduce the flux linkage. In this case, a flux-switching motor is presented, where the magnets are located in the stator, and so is the actuator. By placing a yoke at the top of the magnets, the magnet flux is deviated, and less flux is linked.

Moreover, the number of flux-weakened magnets can be controlled to obtain different magnetisation levels.

The remaining possibility to mechanically vary the flux is to act in the rotor. In [80,81], an actuator is used to control the skew in a two-segment rotor, which can obtain a total magnetisation manipulation range from 0% to 100%. When it comes to [82], an iron plate is placed in the rotor end-plates, deviating the flux through it and achieving the desired result.

In summary, the main drawback of mechanically flux-varying motors is the complexity of the manufacturing process, the associated costs, and the maintenance of the mechanical parts.

3. Analysis of Performance of VF and MP Motors

In this section, different electric motors designs implementing multiphase and variable flux technologies are compared by using FEM simulations. The considered motor designs are the following:

- Three-phase motor.
- Multiphase motor: dual three-phase motor (DTP).
- Variable flux (VF) motor: variable flux memory motor (VFMM).
- Multiphase VF motor: combination of DTP winding and VFMM rotor.

On the one hand, the DTP motor was selected among the MP motors, as it has the benefits of multiphase and three-phase motors and it is a potential candidate for EVs, as mentioned in the literature review. On the other hand, the VFMM was selected as VF motor, as it is the most similar to a conventional permanent magnet motor and is easier to make a fair comparison between them. However, the problem of large magnetising and demagnetising currents is not covered in this article.

To calculate the current amplitude and angle that corresponds to each working point, the motor flux map was built for each motor in the MotorCAD software. The model was built with 7 current amplitude values (0:50:300 Arms), 19 current angle values (0:5:90°), and 180 rotor positions each electric cycle to calculate iron and magnet losses for the efficiency maps accurately.

To perform the comparison between the four motors, the following key performance indicators were evaluated:

- Maximum torque capability: following the MTPA curve of the motors, the maximum torque capability of each motor was calculated at 5000 rpm.
- Maximum power at maximum speed: considering the voltage and current limits, the maximum power at maximum speed of 15,000 rpm was computed.
- Torque ripple: the peak-to-peak torque ripple amplitude with respect to the average torque value was computed in percentages. The torque ripple was computed in 4 characteristic working points over the maximum envelope, which are listed below.
- Efficiency and power losses: efficiency maps were compared in the entire working region. In addition, the power loss distribution was calculated in the four selected working points.

As mentioned above, four characteristic working points were selected to compare the torque ripple and losses of the motor (illustrated in Figure 4):

- WP1: 5000 rpm and 300 Nm. High torque in the MTPA region.
- WP2: 5000 rpm and 90 Nm. Low torque in the MTPA region.
- WP3: 15,000 rpm and 100 Nm. High torque in the FW region.
- WP4: 15,000 rpm and 30 Nm. Low torque in the FW region.

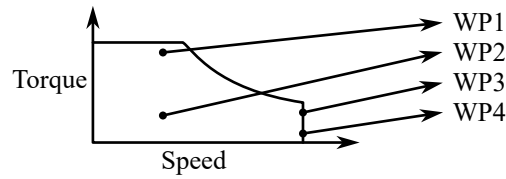


Figure 4. Selected working points for performance comparison.

3.1. Reference Motor

As the reference motor to work with, the automotive three-phase motor in Figure 5 provided by Ansys MotorCAD software was chosen. The meshed FEM simulation model is shown in Figure 5c, which was used to evaluate the motor. It consisted of a distributed winding stator and a rotor with two v-shaped magnet layers. The main characteristics of the motor and the chosen inverter ratings are given in Table 1.

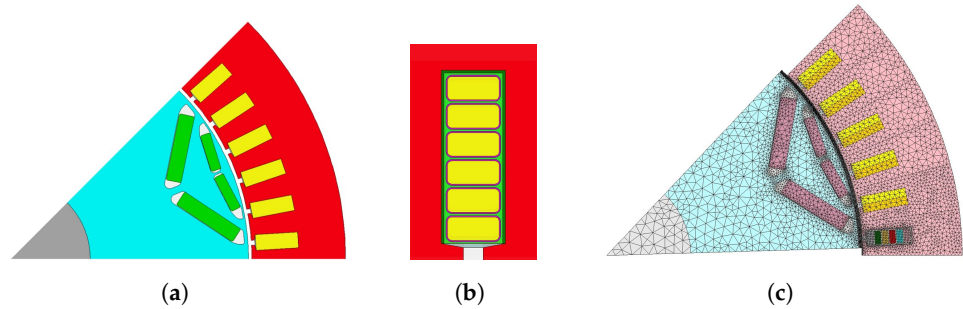


Figure 5. Analysed 3-phase motor. (a) Single pole. (b) Single slot. (c) Meshed FEM model.

Table 1. Parameters of the analysed 3-phase motor.

| Motor Parameters | Value | Winding Parameters | Value |
|------------------------|------------|---------------------|-------|
| Slots/Pole pairs | 48/4 | Phase number | 3 |
| Maximum motor speed | 15,000 rpm | Conductors per slot | 6 |
| Maximum DC bus voltage | 720 V | Parallel paths | 2 |
| Maximum current | 300 Arms | Turns per phase | 24 |

The winding layout of the 3-phase motor is illustrated in Figure 6 together with the corresponding star of slots. The winding characteristics are also gathered in Table 1.

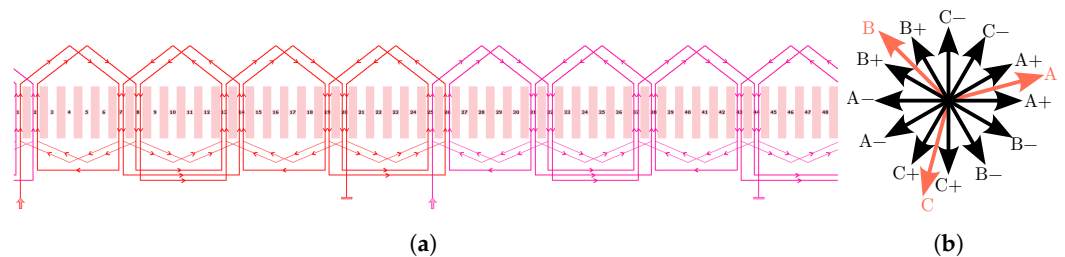


Figure 6. Winding layout and star of slots of the 3-phase motor. (a) Winding layout. (b) Star of slots.

To calculate the winding factor, starting from the star of slots in Figure 6b, the sum of the phase vectors was performed and a value of 0.965 was obtained ($K_w = \cos(15^\circ) = 0.9659$). This means that 96.59% of the flux is linked in the stator winding.

3.2. Multiphase Winding Configuration

To achieve a comparable MP motor, the DTP stator winding configuration was chosen, as regarding the literature analysis, it seemed to be one of the best choices considering the advantages and challenges of MP motors. Starting from the reference three-phase motor, to change the number of phases from 3 to 6, the winding pattern in Figure 6 was changed to

the one in Figure 7. Unlike the winding factor in the three-phase motor, which has a value of 0.9659, the one in the DTP winding is one ($K_w = 1$). This permits linking all the flux.

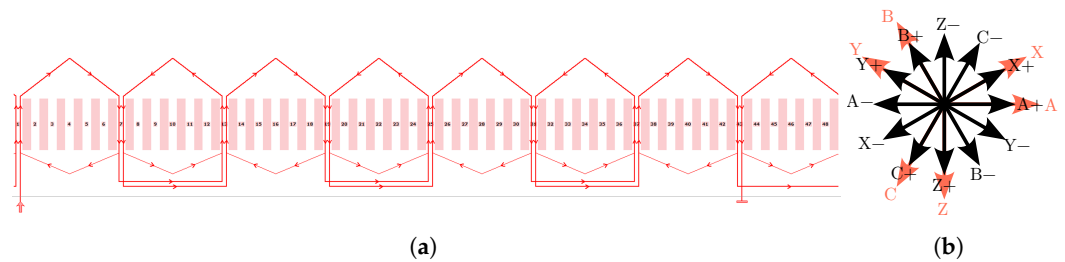


Figure 7. Winding layout and star of slots of the DTP motor. (a) Winding layout. (b) Star of slots.

When it comes to the neutral points of the DTP motor, the two-neutral-point configuration was selected. The independent neutral points allowed for maximising the DC bus voltage utilisation to the same extent of the three-phase motor. Additionally, the inverter current was adjusted to half of the three-phase motor. This way, with the voltage rating the same and the phase number double, the overall power is preserved.

3.3. Variable Flux Rotor

To achieve a variable flux motor, the VFMM was selected as it permits one to obtain a VF motor without adding any extra elements such as coils. The rotor was modified as in Figure 8: the inner magnets were considered as constant flux magnets, whereas the outer magnets were considered as low-coercivity variable flux magnets. These last were considered as fully magnetised (remnant flux density of 1.31 T) in Flux-Enhanced Magnetisation State (FE-MS), and half magnetised (0.655 T) in Flux-Weakened Magnetisation State (FW-MS). Note that the magnetisation and demagnetisation processes are not covered in this paper.

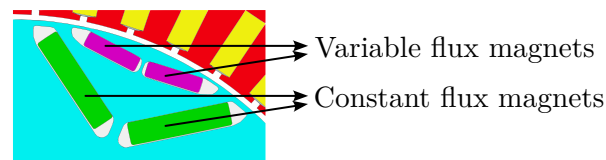


Figure 8. Single pole of the VF motor with the different magnet types.

To define the magnetisation state (MS) of the VF motors in all the working range, the efficiency maps of the FE-MS and FW-MS motors were compared. In each working point, the selected magnetisation state is the one that achieves the highest efficiency. In this section, the 3-phase VF motor is taken as example.

The efficiency maps of the 3-phase VF motor in FE-MS and FW-MS are shown in Figure 9a and 9b, respectively. By comparing both maps and choosing the most efficient MS in each working point, the MS map in Figure 9c was obtained. The FE-MS is more efficient, especially in the low-speed area (except at low loads), as with a higher magnet flux, less current is needed to achieve the required torque, this way decreasing the copper losses. At very low loads, the higher magnetic losses limit the efficiency of the FE-MS. At high speed, a flux-weakening current component needs to be applied to operate inside the voltage limit. This current is higher in the FE-MS, which makes it more efficient to operate in the FW-MS in this region. The overall efficiency map of the 3-phase VF motor is shown in Figure 9d. The same methodology to define the MS was followed in the DTP VF motor.

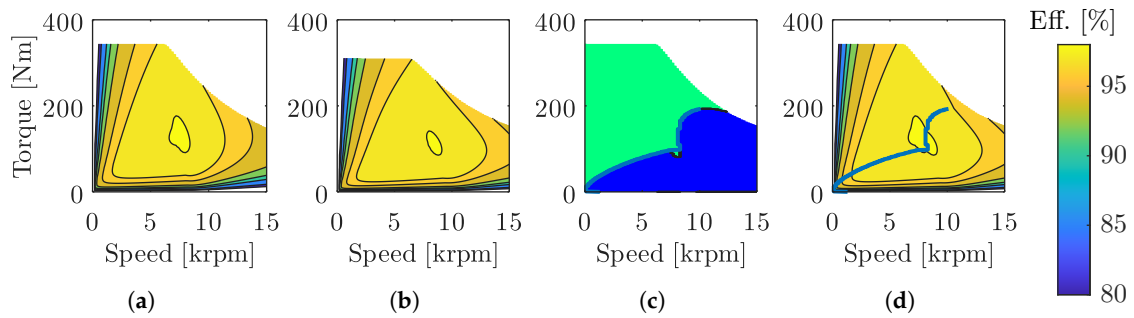


Figure 9. Efficiency maps of the 3-phase VF motor at different magnetisation states and overall efficiency map. (a) FE-MS. (b) FW-MS. (c) Chosen MS. (d) Combination.

4. Results and Discussion

4.1. Torque–Speed Envelope

When evaluating motor performance, maximum torque and constant power are important factors. The maximum torque–speed envelopes of the motors are shown in Figure 10 and summarised in Table 2. The results are discussed taking as reference the conventional three-phase motor.

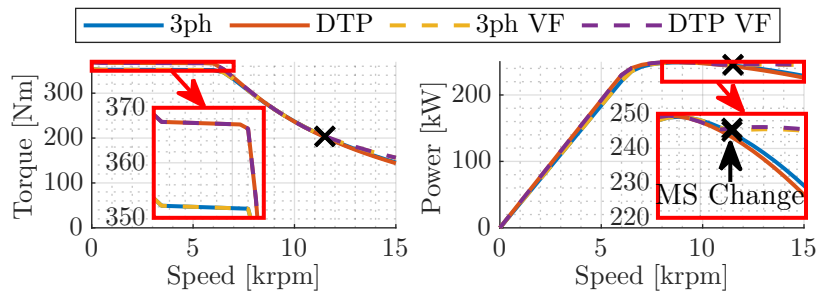


Figure 10. Maximum torque- and power-speed envelopes.

Table 2. Maximum torque and power at maximum speed in the analysed motors.

| | 3-Phase | DTP | 3-Phase VF | DTP VF |
|--------------------------|--------------|---------------|---------------|---------------|
| Maximum torque [Nm] | 353.6 (100%) | 368.8 (+4.3%) | 353.6 (+0%) | 368.8 (+4.3%) |
| Maximum speed power [kW] | 228.8 (100%) | 226.1 (−1.2%) | 245.1 (+7.1%) | 245.5 (+7.3%) |

According to Table 2, the maximum torque capability of both DTP motors was increased by 4.3% compared to the 3-phase ones, which was thanks to the higher winding factor. The VF rotor had no effect on this characteristic, as the VF motors are fully magnetised in this region. When it comes to the constant power region, the DTP motor had a slightly lower power capability at maximum speed compared to the 3-phase one due to the need of a higher FW current. In addition, both VF motors obtained a significant improvement in this region. Once these motors start operating in FW-MS mode, the need for FW current reduces, which allows it to increase the torque-producing current. The power capability increased over 7% in both VF motors at maximum speed.

4.2. Torque Ripple

The torque ripple was calculated in the aforementioned working points, considering low speed, high speed, low torque, and high torque. The torque ripple waveforms are shown in Figure 11, while the numeric values are collected in Table 3. The percentage values refer to the peak-to-peak amplitude with respect to the average value.

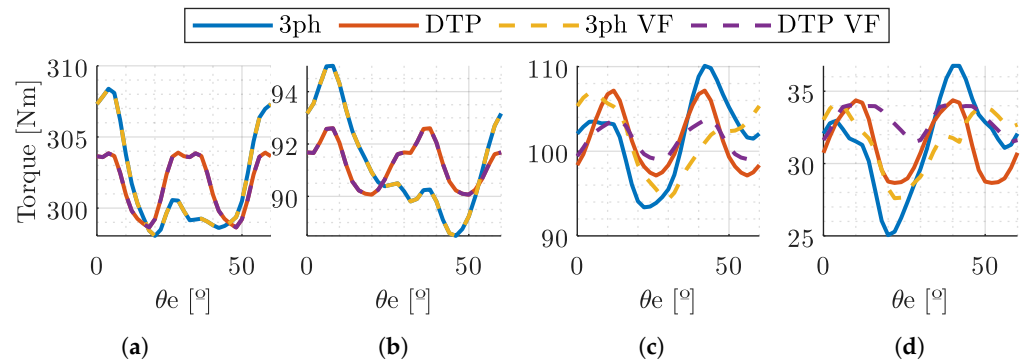


Figure 11. Torque ripple at different working points in 1/6 of the electrical period. (a) WP1. (b) WP2. (c) WP3. (d) WP4.

Table 3. Torque ripple values at different motors and working points.

| | 3-Phase | DTP | 3-Phase VF | DTP VF |
|-----|---------|-------|------------|--------|
| WP1 | 3.4% | 1.7% | 3.4% | 1.7% |
| WP2 | 7.1% | 2.8% | 7.1% | 2.8% |
| WP3 | 16.5% | 9.9% | 12.4% | 4.6% |
| WP4 | 37.3% | 18.2% | 21.4% | 11.8% |

Regarding Table 3, the DTP motors had the smallest torque ripples in all the working points. The 6th order was the first torque ripple harmonic in the 3-phase motors, and the 12th in DTP ones. Eliminating the 6th order harmonic was the main reason why DTP motors had lower torque ripples. With regard to the VF motors, they also showed a reduction in torque ripple in the FW-MS. The reason for this could be the smaller PM field and stator current.

4.3. Power Losses and Efficiency

As well as torque ripple, power losses were calculated at the four working points, where the copper, stator iron, rotor iron, and magnet losses were distinguished. Other losses, such as mechanical ones, were not analysed as they were equal for all motors. The losses are represented in Figure 12 and Table 4.

In WP1, where the torque level is high and the speed is 1/3 of its maximum value, the copper losses were dominant due to the high current. As mentioned in Section 4.1, the DTP motor has more torque capability and needs less current to generate a certain torque level. Thus, the copper losses of the DTP motors were reduced by 7.66% compared to the 3-phase ones. The stator iron losses exhibited minimal variation across the different motor topologies and were the second-highest losses. The rotor iron and magnet losses constituted less than 1% of the total losses in all motors. Notably, the DTP motor demonstrated lower rotor iron and magnet losses compared to the 3-phase motors, which can be attributed to the reduced harmonic content in its airgap field.

In WP2, copper losses had relatively small values due to the low torque at this point, and the stator iron losses were greater than them. When comparing the losses in different motors, they behaved as in WP1: copper, rotor iron, and magnet losses were smaller in the DTP motors for the same reason, whereas there was practically no change in stator iron losses.

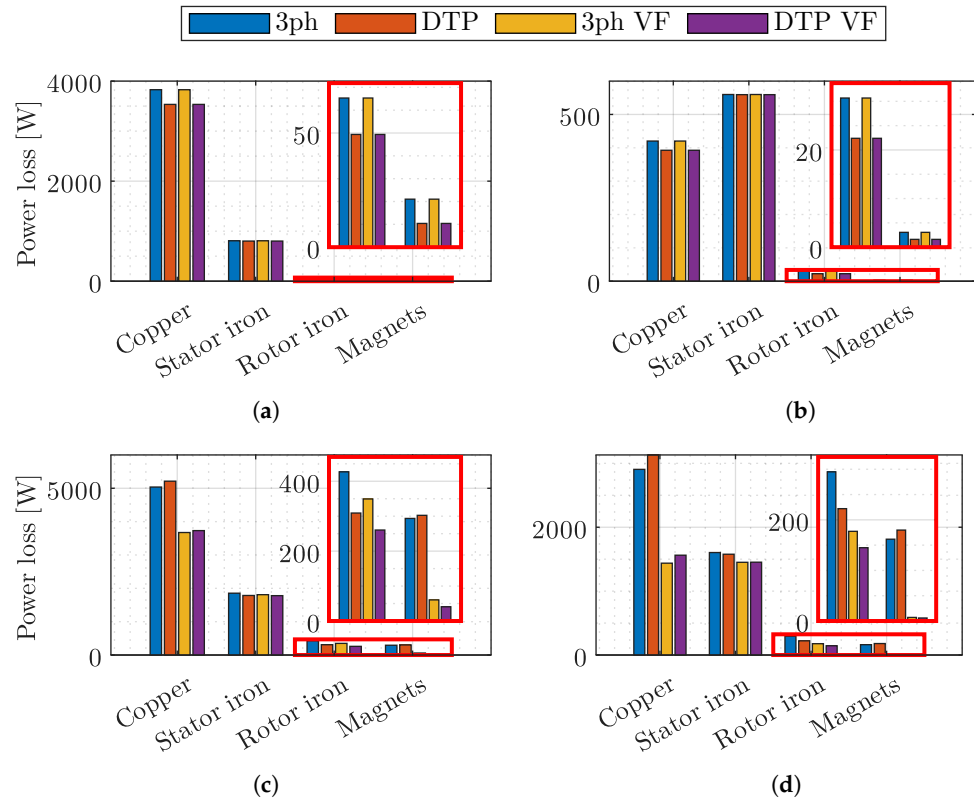


Figure 12. Power loss distribution at different working points. (a) WP1. (b) WP2. (c) WP3. (d) WP4.

Table 4. Power losses at different motors and working points.

| | | 3-Phase | DTP | 3-Phase VF | DTP VF |
|----------------|-------------|---------|--------|------------|--------|
| WP1 Losses [W] | Copper | 3.83 k | 3.53 k | 3.83 k | 3.53 k |
| | Stator iron | 808 | 802 | 808 | 802 |
| | Rotor iron | 65.3 | 49.4 | 65.3 | 49.4 |
| | Magnets | 21 | 10.4 | 21 | 10.4 |
| WP2 Losses [W] | Copper | 420 | 393 | 420 | 393 |
| | Stator iron | 560 | 559 | 560 | 559 |
| | Rotor iron | 30.7 | 22.4 | 30.7 | 22.4 |
| | Magnets | 3.05 | 1.61 | 3.05 | 1.61 |
| WP3 Losses [W] | Copper | 5.04 k | 5.21 k | 3.67 k | 3.73 k |
| | Stator iron | 1.85 k | 1.79 k | 1.81 k | 1.78 k |
| | Rotor iron | 427 | 309 | 349 | 260 |
| | Magnets | 293.6 | 302.5 | 60.4 | 40.7 |
| WP4 Losses [W] | Copper | 2.91 k | 3.13 k | 1.44 k | 1.56 k |
| | Stator iron | 1.6 k | 1.58 k | 1.45 k | 1.45 k |
| | Rotor iron | 295 | 222 | 177 | 145 |
| | Magnets | 162 | 180 | 7.09 | 5.97 |

In WP3, characterised by high torque and speed, copper losses remained predominant. However, there was a notable increase in stator iron, rotor iron, and magnet losses, particularly in the stator iron losses. This increase is attributed to the higher frequency, which elevates iron losses and magnet eddy currents. Compared to the 3-phase motor, the DTP motor exhibited higher copper losses due to the increased current required in the flux-weakening region. Conversely, both VF motors experienced a significant reduction in copper losses (over 25%) because the flux-weakening current requirement is diminished in the FW-MS. Stator iron losses were similar again, but rotor iron and magnet losses were different in the four motors. On the one hand, losses were lower in the DTP topologies due to the more sinusoidal airgap field. On the other hand, as a lower current was required in

the VF topologies, the stator magnetic field was reduced, which lowered the losses in the rotor elements.

Last, in the WP4, torque level is low and the speed is high. The high speed requires a high current to work in the flux-weakening region. In the variable flux motors, this flux-weakening current requirement was lower than in the constant flux motors, reducing copper losses to around 50%. Stator iron losses did not vary significantly, although the VF motors exhibit around 9% lower loss, probably due to the weaker magnetic fields. Rotor iron losses were reduced in both DTP and VF configurations, and the VF modification achieved a higher reduction. Regarding magnet losses, the DTP motor had slightly higher losses than the 3-phase motor. Although the DTP motor produces a field with less harmonic content, which should reduce magnet losses, it seems that the higher stator current used for field-weakening counters this advantage, generating even more losses than in the 3-phase motor. Additionally, it can be observed that in the VF configurations, magnet losses were drastically reduced by more than 95%, which further justifies the pronounced effect of the field-weakening current in these losses.

4.4. Overall Performance

To sum up, all the indicators mentioned are summarised in Figure 13.

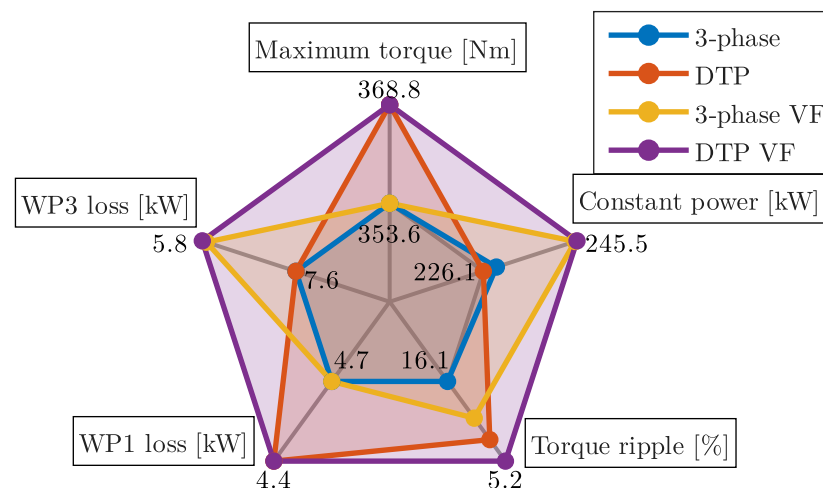


Figure 13. Overall summary of motor performances.

Figure 13 shows that the 3-phase motor had the worst overall performance while the DTP VF motor was the one with the best performance. The maximum torque capability was superior in both DTP motors, while the constant power was enhanced in the VF ones.

When giving the torque ripple values, the average torque ripple of all working points was calculated. The average torque ripple was the best in the DTP VF motor, followed by the DTP and the VF, which also showed improvement compared to the 3-phase one. Regarding losses, only WP1 (low speed) and WP3 (high speed) were represented, as the loss difference between the motors was mainly dependent on speed. The DTP motors showed better performance at low speed (WP1), whereas the VF motors showed better results at high speed (WP3).

5. Conclusions

In this paper, three different motor technologies are compared: multiphase, variable flux, and conventional 3-phase motors. As a result, the benefits and drawbacks of each technologies are identified. First, a literature review is conducted to identify their characteristics, advantages, and drawbacks. This review is complemented by FEM simulations of 3-phase, DTP, 3-phase VF, and DTP VF motors, which demonstrate their characteristics. The main contribution is that both technologies have been implemented in a single motor

to evaluate and quantify their impact together, obtaining higher torque and constant power values, lower torque ripples, and higher efficiencies in the whole working range.

According to the literature review, MP motors have inherent advantages, such as reduced torque ripple, higher torque capability, power segmentation, and the need of a smaller DC-link capacitance in the inverter, increasing the power density of the whole system. Torque levels are improved around 3% just by increasing the phase number, and torque ripple reduces from around 20% until 60% in the mentioned articles, which is a significant improvement. Power losses are also decreased: the copper loss decrease thanks to higher winding factors could benefit from 3% higher efficiencies in a driving cycle, and iron and rotor (magnet and iron) losses reduced around 25% and 50%, respectively. Moreover, there are additional degrees of freedom when controlling the motor, which could be used to enhance its performance even more.

Concerning VF motors, HE motors have good controllability and flux-weakening performance, but the need for additional coils and converters makes the manufacturing process more complex and more expensive, which is a significant drawback for EVs. Moreover, in the cases that slip rings are used to transfer energy to the rotor, there is more need for maintenance. VFMMs are a very interesting choice, but the high magnetising currents require an oversized inverter, which is the major challenge to introduce this technology to EVs. Last, among mechanically flux-varying motors, the ones that use the centrifugal force of the rotor are identified as the most attractive, as they do not require additional actuators. However, the complex flux-varying technologies can elevate the manufacturing costs.

Regarding the FEM simulations, the following general conclusions are obtained. All the comparative indicators are given with respect to the reference three-phase motor.

- The DTP winding improved the maximum torque capability by 4.3% thanks to the higher winding factor. This also reduces the copper losses in the low speed region between 6% and 8%, and magnet and rotor losses between 25% and 50%, although they are not significant. At maximum speed, the need for higher flux-weakening currents increased copper losses between 3% and 8%, but stator iron losses reduced between 1% and 4%, which could be thanks to the more sinusoidal MMF. Last, rotor losses reduced around 25% for the same reason but magnet losses increased between 1% and 3% because of the larger flux-weakening current. Regarding torque ripple, it was reduced more than 40% at all the working points.
- The VF rotor had the same performance at low speed, as in the FE-MS the magnets were fully magnetised, same as in the three-phase motor. Therefore, the benefits came at high speeds when FW-MS was used to weaken magnet flux. This improved the maximum-speed power capability by 7.1% as less amount of current was used to weaken magnet flux. The smaller current and magnetic fields also reduced all losses, accounting for 23% and 38% total loss reductions in the high-speed working points, which was a significant improvement. Furthermore, torque ripple was also reduced at these points by 25% and 43% for the same reason.
- The DTP VF motor exhibited advantages of both DTP and VF motors, being the best candidate among all the motors analysed. The maximum torque was increased by 4.3% and the power at maximum speed by 7.3%. The overall losses were reduced between 3.5% and 7% in the low-speed region and between 23% and 37% in the high-speed one, improving the efficiency in the whole working range. Torque ripple was also reduced between 40% and 50% in the low-speed region and around 70% at high speeds, which is a huge improvement.

The study demonstrated that the advantages of VF and MP motors can be combined to improve the motor performance significantly in the whole operating region. However, the magnetisation and demagnetisation currents of the VFMMs were not analysed, which could be very high as identified in the literature references. Moreover, the coercivity of the magnets was not considered, thus disregarding the unwanted on-load demagnetisation of the magnets. These two aspects are the main constraints to achieve competitive VFMMs.

Although the effectiveness of the multiphase variable flux memory motor was reported, further work is needed considering the mentioned points.

Author Contributions: Conceptualization, B.A., G.A. and A.E.; methodology, B.A., G.A. and A.E.; formal analysis, B.A.; investigation, B.A., G.A., A.E. and P.M.; data curation, B.A. and I.I.; writing—original draft preparation, B.A.; writing—review and editing, B.A., G.A., A.E., P.M. and I.I.; supervision, G.A. and A.E.; project administration, G.A.; funding acquisition, G.A., A.E., P.M. and I.I. All authors have read and agreed to the published version of the manuscript.

Funding: This work was funded by the Basque Government under: ELKARTEK reference KK-2023/00091, and Non-Doctoral Research Staff Training Programme grants PRE-2022-1-0137 and PRE-2023-2-0287.

Institutional Review Board Statement: Not applicable.

Informed Consent Statement: Not applicable.

Data Availability Statement: The data presented in this study are available on request from the corresponding author.

Conflicts of Interest: The authors declare no conflicts of interest.

References

- Okamura, M.; Takaoka, T. The Evolution of Electric Components in Prius. *IEEE J. Ind. Appl.* **2022**, *11*, 21007126. [\[CrossRef\]](#)
- Cheng, M.; Chan, C. General Requirement of Traction Motor Drives. In *Encyclopedia of Automotive Engineering*; Wiley: Chichester, UK, 2014; pp. 1–18. [\[CrossRef\]](#)
- Morya, A.K.; Gardner, M.C.; Anvari, B.; Liu, L.; Yepes, A.G.; Doval-Gandoy, J.; Toliyat, H.A. Wide Bandgap Devices in AC Electric Drives: Opportunities and Challenges. *IEEE Trans. Transp. Electrification* **2019**, *5*, 3–20. [\[CrossRef\]](#)
- El Hadraoui, H.; Zegrari, M.; Chebak, A.; Laayati, O.; Guennouni, N. A Multi-Criteria Analysis and Trends of Electric Motors for Electric Vehicles. *World Electr. Veh. J.* **2022**, *13*, 65. [\[CrossRef\]](#)
- Sokolov, E. Comparative study of electric car traction motors. In Proceedings of the 2017 15th International Conference on Electrical Machines, Drives and Power Systems (ELMA), Sofia, Bulgaria, 1–3 June 2017; pp. 348–353. [\[CrossRef\]](#)
- Nekoubin, A.; Soltani, J.; Dowlatshahi, M. Comparative Analysis of Three-phase and Five-phase Permanent-magnet Motor Based on Finite Element Method. *J. Electr. Eng. Technol.* **2020**, *15*, 1705–1712. [\[CrossRef\]](#)
- Jin, L.; Norrga, S.; Zhang, H.; Wallmark, O. Evaluation of a multiphase drive system in EV and HEV applications. In Proceedings of the 2015 IEEE International Electric Machines & Drives Conference (IEMDC), Coeur d’Alene, ID, USA, 10–13 May 2015; pp. 941–945. [\[CrossRef\]](#)
- Tang, G.; Kong, W.; Zhang, T. The Investigation of Multiphase Motor Fault Control Strategies for Electric Vehicle Application. *J. Electr. Eng. Technol.* **2020**, *15*, 163–177. [\[CrossRef\]](#)
- Wu, S.; Zhou, J.; Zhang, X.; Yu, J. Design and Research on High Power Density Motor of Integrated Motor Drive System for Electric Vehicles. *Energies* **2022**, *15*, 3542. [\[CrossRef\]](#)
- Frikha, M.A.; Croonen, J.; Deepak, K.; Benomar, Y.; El Baghdadi, M.; Hegazy, O. Multiphase Motors and Drive Systems for Electric Vehicle Powertrains: State of the Art Analysis and Future Trends. *Energies* **2023**, *16*, 768. [\[CrossRef\]](#)
- Salem, A.; Narimani, M. A Review on Multiphase Drives for Automotive Traction Applications. *IEEE Trans. Transp. Electrification* **2019**, *5*, 1329–1348. [\[CrossRef\]](#)
- Keller, D.; Kuenzler, M.; Karayel, A.; Werner, Q.; Parspour, N. Potential of Dual Three-Phase PMSM in High Performance Automotive Powertrains. In Proceedings of the 2020 International Conference on Electrical Machines (ICEM), Gothenburg, Sweden, 23–26 August 2020; pp. 1800–1806. [\[CrossRef\]](#)
- Tsunata, R.; Yokomichi, K.; Takemoto, M.; Imai, J. Design and Analysis of Hybrid-Excitation Variable Flux Memory Motor for Traction Applications: Improving Output Power in High-Speed Area During Six-Step Operation Mode. *IEEE Access* **2023**, *11*, 82024–82036. [\[CrossRef\]](#)
- Kim, J.M.; Choi, J.Y.; Lee, K.S.; Lee, S.H. Design and Analysis of Surface-Mounted-Type Variable Flux Permanent Magnet Motor for Wide-Speed Range Applications. *IEEE Trans. Magn.* **2015**, *51*, 1–4. [\[CrossRef\]](#)
- Fukushige, T.; Limsuwan, N.; Kato, T.; Akatsu, K.; Lorenz, R.D. Efficiency Contours and Loss Minimization Over a Driving Cycle of a Variable Flux-Intensifying Machine. *IEEE Trans. Ind. Appl.* **2015**, *51*, 2984–2989. [\[CrossRef\]](#)
- Gholamian, M.; Beik, O.; Arshad, M. A Review of State-of-the-Art Multiphase and Hybrid Electric Machines. *Electronics* **2024**, *13*, 3636. [\[CrossRef\]](#)
- Zhang, G.; Hua, W.; Cheng, M.; Liao, J. Design and Comparison of Two Six-Phase Hybrid-Excited Flux-Switching Machines for EV/HEV Applications. *IEEE Trans. Ind. Electron.* **2016**, *63*, 481–493. [\[CrossRef\]](#)
- Al-Adsani, A.S.; Beik, O. Design of a Multiphase Hybrid Permanent Magnet Generator for Series Hybrid EV. *IEEE Trans. Energy Convers.* **2018**, *33*, 1499–1507. [\[CrossRef\]](#)
- Levi, E. Multiphase Electric Machines for Variable-Speed Applications. *IEEE Trans. Ind. Electron.* **2008**, *55*, 1893–1909. [\[CrossRef\]](#)

20. Janaszek, M. Structures of vector control of n-phase motor drives based on generalized Clarke transformation. *Bull. Pol. Acad. Sci. Tech. Sci.* **2016**, *64*, 865–872. [[CrossRef](#)]
21. Parsa, L. On advantages of multi-phase machines. In Proceedings of the 31st Annual Conference of IEEE Industrial Electronics Society, Raleigh, NC, USA, 6–10 November 2005; p. 6. [[CrossRef](#)]
22. Cai, W.; Wu, X.; Zhou, M.; Liang, Y.; Wang, Y. Review and Development of Electric Motor Systems and Electric Powertrains for New Energy Vehicles. *Automot. Innov.* **2021**, *4*, 3–22. [[CrossRef](#)]
23. Xue, Y.; Lu, J.; Wang, Z.; Tolbert, L.M.; Blalock, B.J.; Wang, F. A compact planar Rogowski coil current sensor for active current balancing of parallel-connected Silicon Carbide MOSFETs. In Proceedings of the 2014 IEEE Energy Conversion Congress and Exposition (ECCE), Pittsburgh, PA, USA, 14–18 September 2014; pp. 4685–4690. [[CrossRef](#)]
24. Yadav, G.; Nag, S.S. Review of Factors Affecting Current Sharing and Techniques for Current Balancing in Paralleled Wide Bandgap Devices. In Proceedings of the 2020 3rd International Conference on Energy, Power and Environment: Towards Clean Energy Technologies, Shillong, India, 5–7 March 2021; pp. 1–6. [[CrossRef](#)]
25. Taha, W.; Azer, P.; Callegaro, A.D.; Emadi, A. Multiphase Traction Inverters: State-of-the-Art Review and Future Trends. *IEEE Access* **2022**, *10*, 4580–4599. [[CrossRef](#)]
26. Michieletto, D.; Bianchi, N.; Brunetti, M. Dual Three-phase Motor Fault Tolerance for Modern Transport. In Proceedings of the 2021 International Aegean Conference on Electrical Machines and Power Electronics (ACEMP) & 2021 International Conference on Optimization of Electrical and Electronic Equipment (OPTIM), Brasov, Romania, 2–3 September 2021; pp. 405–412. [[CrossRef](#)]
27. Wang, S.; Zhu, Z.; Pride, A.; Shi, J.; Deodhar, R.; Umemura, C. Comparison of Different Winding Configurations for Dual Three-Phase Interior PM Machines in Electric Vehicles. *World Electr. Veh. J.* **2022**, *13*, 51. [[CrossRef](#)]
28. Abdel-Khalik, A.S.; Ahmed, S.; Massoud, A.M. Low Space Harmonics Cancellation in Double-Layer Fractional Slot Winding Using Dual Multiphase Winding. *IEEE Trans. Magn.* **2015**, *51*, 1–10. [[CrossRef](#)]
29. Parsa, L.; Toliyat, H. Multi-phase permanent magnet motor drives. In Proceedings of the 38th IAS Annual Meeting on Conference Record of the Industry Applications Conference, Salt Lake City, UT, USA, 12–16 October 2003; Volume 1, pp. 401–408. [[CrossRef](#)]
30. Arribas, B.; Almandoz, G.; Egea, A.; Poza, J.; Iturbe, I. Analysis of Multiphase Permanent Magnet Motors via Space-Harmonic Model. In Proceedings of the 2024 International Conference on Electrical Machines (ICEM), Torino, Italy, 1–4 September 2024; pp. 1–7. [[CrossRef](#)]
31. Diana, M.; Ruffo, R.; Guglielmi, P. Low torque ripple tooth coil windings multi-3-phase machines: Design considerations and validation. *IET Electr. Power Appl.* **2020**, *14*, 262–273. [[CrossRef](#)]
32. Zhang, J.; He, S.J.; Wang, K. Multi-Harmonic Currents Control Strategy for Five-Phase Permanent Magnet Machine with non-sinusoidal back-EMF. *IEEE Access* **2020**, *1*. [[CrossRef](#)]
33. Wang, J.; Qu, R.; Zhou, L. Dual-Rotor Multiphase Permanent Magnet Machine With Harmonic Injection to Enhance Torque Density. *IEEE Trans. Appl. Supercond.* **2012**, *22*, 5202204. [[CrossRef](#)]
34. Hu, Y.; Zhu, Z.Q.; Odavic, M. Torque Capability Enhancement of Dual Three-Phase PMSM Drive With Fifth and Seventh Current Harmonics Injection. *IEEE Trans. Ind. Appl.* **2017**, *53*, 4526–4535. [[CrossRef](#)]
35. Wang, K.; Zhu, Z.Q.; Ren, Y.; Ombach, G. Torque Improvement of Dual Three-Phase Permanent-Magnet Machine With Third-Harmonic Current Injection. *IEEE Trans. Ind. Electron.* **2015**, *62*, 6833–6844. [[CrossRef](#)]
36. Sculler, F.; Becker, F.; Zahr, H.; Semail, E. Design of a Bi-Harmonic 7-Phase PM Machine with Tooth-Concentrated Winding. *IEEE Trans. Energy Convers.* **2020**, *35*, 1567–1576. [[CrossRef](#)]
37. Wang, J.; Zhou, L.; Qu, R. Harmonic current effect on torque density of a multiphase permanent magnet machine. In Proceedings of the 2011 International Conference on Electrical Machines and Systems, Beijing, China, 20–23 August 2011; pp. 1–6. [[CrossRef](#)]
38. Cervone, A.; Slunjski, M.; Levi, E.; Brando, G. Optimal Third-Harmonic Current Injection for Asymmetrical Multiphase Permanent Magnet Synchronous Machines. *IEEE Trans. Ind. Electron.* **2021**, *68*, 2772–2783. [[CrossRef](#)]
39. Wang, K. Effects of Harmonics Into Magnet Shape and Current of Dual Three-Phase Permanent Magnet Machine on Output Torque Capability. *IEEE Trans. Ind. Electron.* **2018**, *65*, 8758–8767. [[CrossRef](#)]
40. Wang, K.; Zhu, Z.Q.; Ombach, G. Torque Improvement of Five-Phase Surface-Mounted Permanent Magnet Machine Using Third-Order Harmonic. *IEEE Trans. Energy Convers.* **2014**, *29*, 735–747. [[CrossRef](#)]
41. Dwari, S.; Parsa, L. An Optimal Control Technique for Multiphase PM Machines Under Open-Circuit Faults. *IEEE Trans. Ind. Electron.* **2008**, *55*, 1988–1995. [[CrossRef](#)]
42. Mohammadpour, A.; Mishra, S.; Parsa, L. Fault-Tolerant Operation of Multiphase Permanent-Magnet Machines Using Iterative Learning Control. *IEEE J. Emerg. Sel. Top. Power Electron.* **2014**, *2*, 201–211. [[CrossRef](#)]
43. Liu, Z.; Li, Y.; Zheng, Z. A review of drive techniques for multiphase machines. *CES Trans. Electr. Mach. Syst.* **2018**, *2*, 243–251. [[CrossRef](#)]
44. Liu, Z.; Zheng, Z.; Li, Y. Enhancing Fault-Tolerant Ability of a Nine-Phase Induction Motor Drive System Using Fuzzy Logic Current Controllers. *IEEE Trans. Energy Convers.* **2017**, *32*, 759–769. [[CrossRef](#)]
45. Levi, E.; Jones, M.; Vukosavic, S.; Toliyat, H. Operating Principles of a Novel Multiphase Multimotor Vector-Controlled Drive. *IEEE Trans. Energy Convers.* **2004**, *19*, 508–517. [[CrossRef](#)]
46. Huang, J.; Wang, X.; Sun, Z. Variable flux memory motors: A review. In Proceedings of the 2014 IEEE Conference and Expo Transportation Electrification Asia-Pacific (ITEC Asia-Pacific), Beijing, China, 31 August–3 September 2014; pp. 1–6. [[CrossRef](#)]

47. Zhou, Z.; Hua, H.; Zhu, Z. Flux-Adjustable Permanent Magnet Machines in Traction Applications. *World Electr. Veh. J.* **2022**, *13*, 60. [[CrossRef](#)]
48. Owen, R.; Zhu, Z.Q.; Wang, J.B.; Stone, D.A.; Urquhart, I. Review of variable-flux permanent magnet machines. In Proceedings of the 2011 International Conference on Electrical Machines and Systems, Beijing, China, 20–23 August 2011; pp. 1–6. [[CrossRef](#)]
49. Toba, A.; Daikoku, A.; Nishiyama, N.; Yoshikawa, Y.; Kawazoe, Y. Recent technical trends in variable flux motors. In Proceedings of the 2014 International Power Electronics Conference (IPEC-Hiroshima 2014—ECCE ASIA), Hiroshima, Japan, 18–21 May 2014; pp. 2011–2018. [[CrossRef](#)]
50. Zhu, Z.Q.; Cai, S. Hybrid excited permanent magnet machines for electric and hybrid electric vehicles. *CES Trans. Electr. Mach. Syst.* **2019**, *3*, 233–247. [[CrossRef](#)]
51. Cinti, L.; Bianchi, N. Hybrid-Excited PM Motor for Electric Vehicle. *Energies* **2021**, *14*, 916. [[CrossRef](#)]
52. Huang, L.; Zhu, Z.; Chu, W. Optimization of electrically excited synchronous machine for electrical vehicle applications. In Proceedings of the 8th IET International Conference on Power Electronics, Machines and Drives (PEMD 2016), Glasgow, UK, 19–21 April 2016; p. 6. [[CrossRef](#)]
53. Contó, C.; Bianchi, N. A Hybrid-Excitation Synchronous Motor with a Change in Polarity. *Machines* **2022**, *10*, 869. [[CrossRef](#)]
54. Amara, Y.; Vido, L.; Gabsi, M.; Hoang, E.; Lecrivain, M.; Chabot, F. Hybrid Excitation Synchronous Machines: Energy Efficient Solution for Vehicle Propulsion. In Proceedings of the 2006 IEEE Vehicle Power and Propulsion Conference, Windsor, UK, 6–8 September 2006; Volume 58, pp. 1–6. [[CrossRef](#)]
55. Di Barba, P.; Bonislawski, M.; Palka, R.; Paplicki, P.; Wardach, M. Design of Hybrid Excited Synchronous Machine for Electrical Vehicles. *IEEE Trans. Magn.* **2015**, *51*, 1–6. [[CrossRef](#)]
56. Hua, H.; Cheng, M.; Zhang, G. A Novel Hybrid Excitation Flux-Switching Motor for Hybrid Vehicles. *IEEE Trans. Magn.* **2009**, *45*, 4728–4731. [[CrossRef](#)]
57. Hoang, E.; Lecrivain, M.; Hlioui, S.; Gabsi, M. Hybrid excitation synchronous permanent magnets synchronous machines optimally designed for hybrid and full electrical vehicle. In Proceedings of the 8th International Conference on Power Electronics—ECCE Asia, Jeju, Republic of Korea, 30 May–3 June 2011; pp. 153–160. [[CrossRef](#)]
58. Gao, Y.; Li, D.; Qu, R.; Fan, X.; Li, J.; Ding, H. A Novel Hybrid Excitation Flux Reversal Machine for Electric Vehicle Propulsion. *IEEE Trans. Veh. Technol.* **2018**, *67*, 171–182. [[CrossRef](#)]
59. Yue, Q.; Liu, G.; Xu, Z.; Xiong, D.; Song, Z. Establishment the equivalent model and parameter calculation of a new concept of high-speed permanent magnet synchronous machine with hybrid excitation on the stator. *Energy Rep.* **2022**, *8*, 815–824. [[CrossRef](#)]
60. Athavale, A.; Erato, D.J.; Lorenz, R.D. Enabling Driving Cycle Loss Reduction in Variable Flux PMSMs Via Closed-Loop Magnetization State Control. *IEEE Trans. Ind. Appl.* **2018**, *54*, 3350–3359. [[CrossRef](#)]
61. Jayarajan, R.; Fernando, N.; Nutkani, I.U. A Review on Variable Flux Machine Technology: Topologies, Control Strategies and Magnetic Materials. *IEEE Access* **2019**, *7*, 70141–70156. [[CrossRef](#)]
62. Badahdah, H.S.; El-Refaie, A. A Review of Recent Topologies of Variable Flux Machines. In Proceedings of the 2024 International Conference on Electrical Machines (ICEM), Torino, Italy, 1–4 September 2024; pp. 1–7. [[CrossRef](#)]
63. Lee, J.I.N.H.; Song, J.y.; Yeo, H.k. Numerical Evaluation of a Concentrated-Winding Variable Flux Memory Motor With a Hybrid Magnet Arrangement. *IEEE Access* **2023**, *11*, 71756–71765. [[CrossRef](#)]
64. Han, M.; Besson, C.; Savary, A.; Becher, Y. Performance Assessment of a Variable-Flux Permanent-Magnet Memory Motor. *Int. J. Electr. Comput. Eng.* **2019**, *13*, 296–303. [[CrossRef](#)]
65. Hua, H.; Zhu, Z.Q.; Pride, A.; Deodhar, R.P.; Sasaki, T. A Novel Variable Flux Memory Machine With Series Hybrid Magnets. *IEEE Trans. Ind. Appl.* **2017**, *53*, 4396–4405. [[CrossRef](#)]
66. Sakai, K.; Yoneda, K.; Suzuki, W. Variable-Magnetization Interior Permanent Magnet Motor Yield Widely Variable Flux due to Small Magnetizing Current and Operating at High Power over a Wide Speed Range. In Proceedings of the 2021 IEEE Energy Conversion Congress and Exposition (ECCE), Vancouver, BC, Canada, 10–14 October 2021; pp. 4205–4212. [[CrossRef](#)]
67. Yang, H.; Lyu, S.; Lin, H.; Zhu, Z.q.; Zheng, H.; Wang, T. A Novel Hybrid-Magnetic-Circuit Variable Flux Memory Machine. *IEEE Trans. Ind. Electron.* **2020**, *67*, 5258–5268. [[CrossRef](#)]
68. Hua, H.; Zhu, Z.; Pride, A.; Deodhar, R.; Sasaki, T. Comparative study of variable flux memory machines with parallel and series hybrid magnets. In Proceedings of the 2017 IEEE Energy Conversion Congress and Exposition (ECCE), Cincinnati, OH, USA, 1–5 October 2017; Volume 8, pp. 3942–3949. [[CrossRef](#)]
69. Limsuwan, N.; Kato, T.; Akatsu, K.; Lorenz, R.D. Design and Evaluation of a Variable-Flux Flux-Intensifying Interior Permanent-Magnet Machine. *IEEE Trans. Ind. Appl.* **2014**, *50*, 1015–1024. [[CrossRef](#)]
70. Liu, X.; Sun, T.; Zou, Y.; Huang, C.; Liang, J. Modelling and analysis of a novel mechanical-variable-flux IPM machine with rotatable magnetic poles. *IET Electr. Power Appl.* **2020**, *14*, 2171–2178. [[CrossRef](#)]
71. Sun, T.; Liu, X.; Zou, Y.; Huang, C.; Liang, J. Design and optimization of a mechanical variable-leakage-flux interior permanent magnet machine with auxiliary rotatable magnetic poles. *CES Trans. Electr. Mach. Syst.* **2021**, *5*, 21–29. [[CrossRef](#)]
72. Liu, X.; Guo, G.; Zhu, W.; Du, L. Comparative design and analysis of a new type of mechanical-variable-flux flux-intensifying interior permanent magnet motor. *Prog. Electromagn. Res. C* **2021**, *111*, 225–239. [[CrossRef](#)]
73. Liang, J.; Liu, D.; Gao, Y.; Yuan, H.; Liu, X. Design and Analysis of a Novel Mechanical Variable Flux Interior Permanent Magnet Synchronous Motor. *Prog. Electromagn. Res. C* **2022**, *123*, 167–179. [[CrossRef](#)]

74. Tessarolo, A.; Mezzarobba, M.; Menis, R. A novel interior permanent magnet motor design with a self-activated flux-weakening device for automotive applications. In Proceedings of the 2012 XXth International Conference on Electrical Machines, Marseille, France, 2–5 September 2012; pp. 2603–2609. [[CrossRef](#)]
75. Liu, X.; Wang, M.; Chen, D.; Xie, Q. A Variable Flux Axial Field Permanent Magnet Synchronous Machine With a Novel Mechanical Device. *IEEE Trans. Magn.* **2015**, *51*, 1–4. [[CrossRef](#)]
76. Liu, W.; Yang, H.; Lin, H. Design and Analysis of a Novel Mechanical-Variable-Flux Stator Consequent-Pole Machine. In Proceedings of the 2019 22nd International Conference on Electrical Machines and Systems (ICEMS), Harbin, China, 11–14 August 2019; pp. 1–6. [[CrossRef](#)]
77. Jiang, M.; Niu, S. Novel Mechanical Flux-Weakening Design of a Spoke-Type Permanent Magnet Generator for Stand-Alone Power Supply. *Appl. Sci.* **2023**, *13*, 2689. [[CrossRef](#)]
78. Zhu, Z.Q.; Al-Ani, M.M.; Liu, X.; Hasegawa, M.; Pride, A.; Deodhar, R. Comparison of alternate mechanically adjusted variable flux switched flux permanent magnet machines. In Proceedings of the 2012 IEEE Energy Conversion Congress and Exposition, ECCE 2012, Raleigh, NC, USA, 15–20 September 2012; pp. 3655–3662. [[CrossRef](#)]
79. Zhu, Z.Q.; Al-Ani, M.M.J.; Liu, X.; Lee, B. A Mechanical Flux Weakening Method for Switched Flux Permanent Magnet Machines. *IEEE Trans. Energy Convers.* **2015**, *30*, 806–815. [[CrossRef](#)]
80. Zhou, G.; Miyazaki, T.; Kawamata, S.; Kaneko, D.; Hino, N. Development of variable magnetic flux motor suitable for electric vehicle. In Proceedings of the The 2010 International Power Electronics Conference—ECCE ASIA, Sapporo, Japan, 21–24 June 2010; pp. 2171–2174. [[CrossRef](#)]
81. Ishii, T.; Nonaka, T.; Oga, S.; Ohto, M. Manufacturing and Control of a Variable Magnetic Flux Motor Prototype with a Mechanical Adjustment Method. *Electr. Eng. Jpn.* **2017**, *199*, 57–66. [[CrossRef](#)]
82. Urquhart, I.; Tanaka, D.; Owen, R.; Zhu, Z.; Wang, J.; Stone, D. Mechanically actuated variable flux IPMSM for EV and HEV applications. *World Electr. Veh. J.* **2013**, *6*, 684–695. [[CrossRef](#)]

Disclaimer/Publisher’s Note: The statements, opinions and data contained in all publications are solely those of the individual author(s) and contributor(s) and not of MDPI and/or the editor(s). MDPI and/or the editor(s) disclaim responsibility for any injury to people or property resulting from any ideas, methods, instructions or products referred to in the content.